# Permeability and Partition Coefficient of Aqueous Sodium Chloride in Soft Contact Lenses

**L. Guan,[1]* M. E. González Jiménez,[1†] C. Walowski,[1‡] A. Boushehri,[1] J. M. Prausnitz,[1] C. J. Radke[1,2]**

[1]*Chemical and Biomolecular Engineering Department, University of California, 101E Gilman, Berkeley, California 94720-1462*
[2]*Vision Science Group, University of California, Berkeley, California 94720*

Received 7 June 2010; accepted 1 September 2010
DOI 10.1002/app.33336
Published online 26 May 2011 in Wiley Online Library (wileyonlinelibrary.com).

**ABSTRACT:** Transport of physiologic saline through soft contact lenses is important to on-eye behavior. Using a specially designed Stokes-diaphragm cell, we measure aqueous NaCl permeabilities through commercial soft contact lenses at 35°C. The permeabilities increase exponentially with the water content of the lenses spanning a range from $10^{-7}$ to $10^{-5}$ cm$^2$/s. Equilibrium partition coefficients are obtained by the back-extraction of lenses initially immersed in 1*M* aqueous NaCl. Partition coefficients also increase with lens water content but over a smaller range, from 0.1 to 0.7. Because the partition coefficient values are smaller than the water content of the lenses, ideal theory is not followed. Donnan exclusion, bound water, and excluded volume are proposed explanations. The diffusion coefficients of aqueous NaCl through soft contact lenses increase with increasing lens water content following free-volume theory. Aqueous NaCl diffusivities in the lower water-content lenses are smaller than the diffusion coefficient of NaCl in water by factors up to 100 indicating very tortuous diffusion paths. © 2011 Wiley Periodicals, Inc. J Appl Polym Sci 122: 1457–1471, 2011

**Key words:** biomaterials; diffusion; hydrogels

## INTRODUCTION

Modern soft contact lenses (SCLs) are designed to provide sufficient oxygen transport to the cornea to maintain ocular health.[1–6] To achieve this goal during extended wear, lens oxygen permeabilities should exceed 100 Barrer.[6] An additional design criterion is that the salt (NaCl) permeability of an aqueous-saturated SCL should exceed about 2–4 $\times$ $10^{-7}$ cm$^2$/s at eye temperature (35°C).[2–7] The stated origin of the salt-permeability criterion is that lens movement on the eye is compromised below this value.[3–7] A lack of lens movement can lead to undesired lens adherence to the cornea. A salt-permeable SCL also permits the exchange of water, electrolytes, and nutrients between the prelens and postlens tear films.

Unfortunately, literature data are sparse for the permeation of sodium chloride at physiologic concentration through SCL materials and rare for SCLs. In 1968, Yasuda et al.[8] measured aqueous NaCl permeabilities ($P$), diffusion coefficients ($D$), and equilibrium partition coefficients ($k$) for crosslinked hydrogels. Yasuda et al.[8] established that the salt diffusivity and partition coefficient increased with rising membrane water content ($w$). The NaCl diffusion coefficient increased monotonically with membrane water content in agreement with free-volume theory, whereas the partition coefficient varied linearly with water volume fraction for high-water-content materials. These results were confirmed over a decade later by Yoon and Jhon,[9,10] who studied a series of hydroxyethyl methacrylate (HEMA)-based membranes of differing crosslink densities. Hamilton et al.[11] and Murphy et al.[12] examined the permeability of a series of aqueous strong electrolytes, including NaCl, through poly(hydroxyethyl methacrylate) (pHEMA) and pHEMA/methyl methacrylate copolymer membranes. These authors confirmed increasing salt permeability with increasing water content of the hydrogel. They further established that ion size and ion and polymer influence on water structure also contribute to salt permeability in hydrogels.[11,12] Following the Ionoflux protocol of Nicolson

*Current address:* School of Materials Science and Engineering, Tianjin University, Tianjin 300072, People's Republic of China.
†*Current address:* Departamento de Ciencias Naturales, Universidad Central, Bogota D. C., Colombia.
‡*Current address:* Institute für Thermodynamik, TK7, Technical University of Berlin, Berlin, Germany.
*Correspondence to:* C.J. Radke, Chemical and Biomolecular Engineering Department, University of California, 101E Gilman, Berkeley, CA 94720-1462 (radke@berkeley.edu).
Contract grant sponsors: China Scholarship Council (to L.G.), Universidad Nacional de Colombia and Colciencias (to M.E.G.J.).

**TABLE I**
**Properties of SCLs**

| Trade name (FDA category)[a] | Material | $w$ (wt %) | $\rho_L$ (g/cm$^3$) | $L$ (μm) |
|---|---|---|---|---|
| Focus Night & Day (I/SiHy) | Lotrafilcon A | 24 | 1.08 | 82 |
| O2 Optix (I/SiHy) | Lotrafilcon B | 33 | 1.08 | 87 |
| PureVision (III/SiHy) | Balafilcon A | 36 | 1.064 | 91 |
| Acuvue Oasys (I/SiHy) | Senofilcon A | 38 | 1.12 | 63 |
| Biomedics 38 (I/H) | Polymacon | 38 | 1.12 | 40 |
| SofLens 38 (I/H) | Polymacon | 38 | 1.12 | 46 |
| Acuvue Advance (I/SiHy) | Galyfilcon A | 47 | 1.12 | 59 |
| Biofinity (I/SiHy) | Comfilcon A | 48 | 1.04 | 119 |
| Clarity $H_2O$ (II/H) | Hioxifilcon D | 54 | 1.12 | 122 |
| Biomedics 55 (IV/H) | Ocufilcon | 55 | 1.062 | 102 |
| Focus Monthly Visitint (IV/H) | Vifilcon A | 55 | 1.12 | 95 |
| Acuvue 2 (IV/H) | Etafilcon A | 58 | 1.05 | 89 |
| SofLens Daily Disposable (II/H) | Hilafilcon B | 59 | 1.12 | 181 |
| Proclear One Day (II/H) | Omafilcon A | 60 | 1.06[b] | 155 |
| Proclear Sphere (II/H) | Omafilcon A | 62 | 1.06[b] | 78 |
| Focus Dailies (II/PVA) | Nelfilcon A | 69 | 1.06 | 107 |
| SofLens One Day (II/H) | Hilafilcon A | 70 | 1.12 | 181 |

[a] I (group I: nonionic, low $w$), II (group II: nonionic, high $w$), III (group III: ionic, low $w$), and IV (group IV: ionic, high $w$) give the FDA categories. H = HEMA; SiHy = siloxane; PVA = polyvinyl alcohol.
[b] Measurements based on a dry density for HEMA of 1.274 (g/cm$^3$)[20] and volume additivity.

et al.,[3] Willis et al.[13] reported aqueous NaCl diffusion coefficients in conventional pHEMA and silicone-hydrogel SCLs. However, because of their measurement procedure, the reported diffusivities, in fact, refer to salt permeabilities. Their results, as those from membrane materials, show that the salt permeabilities of the lenses increase with rising lens water content. In agreement with Hamilton et al.,[11] Willis et al.[13] indicate that below a water content of about 15 wt %, salt permeability declines to zero, suggesting a lack of phase connectivity of water in the hydrogel. Weikart et al.[14] measured the aqueous NaCl permeability of siloxane-based SCLs with various plasma coatings. No effect of the coating was observed.

Austin and Kumar[15] measured the electrical conductivities of aqueous sodium chloride solutions in membranes characteristic of SCLs. They also established that below a critical water content of about 20 wt %, no current conducted, whereas above 20 wt %, the conductivity rose with increasing membrane water content. For a Focus Night & Day (Lotrafilcon A) SCL, the conductivity of aqueous NaCl was five times higher than that in a conventional HEMA-based lens at the same water content. Most recently, Kim et al.[16] measured aqueous salt permeability in silicone-hydrogel membranes for use in drug delivery. They confirmed the essential trend of increasing permeability with rising membrane water content, despite very low aqueous NaCl permeabilities.

The goal of this work was to measure the permeability ($P = Dk$) of physiologic-concentration NaCl in water-saturated commercial SCLs at eye temperature. We employ a modified diaphragm or Stokes cell[9–12,17–19] suitable for small, curved commercial contact lenses. Boundary-layer resistances in the diaphragm cell are taken into account by stirring both the donor and receiving chambers over a range of stirring speeds. Aqueous NaCl partition coefficients were obtained by back-extraction from lenses initially saturated at a known salt concentration ($c$).[8–12,16] The diffusivity of aqueous NaCl in the SCL is then obtained from the measured values of permeability and partition coefficient: $D = P/k$. We report the salt partition coefficient, permeability, and diffusivity for 17 commercial SCLs, including those that are HEMA-based (H) and siloxane-based (SiHy).

## EXPERIMENTAL

### Materials

Commercial SCLs were provided by Con-Cise Contact Lens Co (San Leandro, CA). A lens power of −0.75 Diopter was chosen for each lens to provide a relatively uniform radial thickness. Seventeen commercial SCLs were used: ten conventional hydrogels of differing water contents, six last-generation siloxane hydrogels, and one high-water-content poly(vinyl alcohol) (PVA) hydrogel. Table I gives the properties, brand names, materials, U.S. Food and Drug Administration (FDA) categories, saturated-water contents, and wet densities ($\rho_L$) and thicknesses ($L$) of each SCL type. The water content and wet density values are those reported by the manufacturer unless otherwise noted. The harmonic-mean thickness ($L$) of each lens was measured using an electronic thickness gauge (model ET-3, Rehder Development Co., Castro Valley, CA.), with precision

±2 μm. NaCl was from Fisher Chemical (>99%) and was used as received. Distilled/deionized (DDI) water was obtained from a MilliQ purification system (Bedford, MA) with a resistivity greater than 18.2 MΩcm. All solutions were prepared by weight.

## Methods

### Partition-coefficient determination

The equilibrium partition coefficient of NaCl between a water-saturated SCL and the surrounding aqueous solution was obtained by the method of back-extraction or desorption.[8–12,16] Lenses of known dry mass were soaked in an excess of aqueous salt solution of known initial high concentration ($c_0$), typically 1*M*, and known initial volume ($V_0$) until equilibrium was attained. After equilibration, the lenses were immersed in a volume ($V$) of DDI water. Salt leached into the DDI aqueous phase until equilibrium was reattained at a lower aqueous-phase salt concentration. The partition coefficient ($k$) is defined as the ratio of the equilibrium salt concentration in the lens to that in the surrounding aqueous solution. Provided that $kV_L/V_0 \ll 1$, mass conservation of salt requires that

$$k = \frac{Vc}{V_L c_0[1 - (\alpha + V/V_0)c/c_0]} \quad (1)$$

where $V_L$ is the volume of the lenses and α is the ratio of the salt partition coefficient at concentration ($c$) to that at concentration $c_0$. In all cases studied here, $V/V_0$ was less than 0.1, and $c/c_0$ was very much less than unity. We expect that α for NaCl is, at most, close to unity.[9,10,21,22] Therefore, $(\alpha + V/V_0)c/c_0 \ll 1$. Equation (1) then reduces to the following simple result:

$$k = \frac{Vc}{V_L c_0} \quad (2)$$

This result means that the back-extraction method provides the partition coefficient at the saturating salt concentration ($c_0$). The lens volume follows from additivity:

$$V_L = \frac{m_2}{\rho_L(1 - w)} \quad (3)$$

where $m_2$ is the dry mass of the polymer in the lenses, $w$ is the saturated equilibrium weight fraction of water in the lens (Table I), and $\rho_L$ is the corresponding wet-lens density (Table I).

### Partition-coefficient measurement

The back-extraction technique is simple in principle.[8–12,16] After removal from the high-concentration saturating solution, however, saline solution remaining on the surface of the lens must be blotted quantitatively. Variation in blotting of the small lenses can lead to significant errors among different operators. After considerable effort, the following procedure was adopted.[23] The contact lenses were first immersed in DDI water for at least 2 days to remove packaging-solution additives. Five contact lenses were then equilibrated in approximately 250 mL of a 1*M* aqueous NaCl solution in a constant-temperature bath (VWR 1110 Controller) at 35°C. After 1 day of equilibration, the contact lenses were removed, one at a time, from the 1*M* saturating salt solution and placed with their concave sides facing up on a folded Kimwipe and carefully blotted (several times with a fingertip wrapped with another sheet of Kimwipe). After blotting, the contact lenses were immediately immersed in a known mass of DDI water (ca 20 g) in sealed vials and resubmerged in the constant-temperature bath. From the initial trial measurements, the equilibration time was about 1 day. Subsequent to desorption for at least 2 days, the concentration of the supernatant salt solution was measured by a hand-held Cole Parmer conductivity cell (Cole Parmer # 19820-00, Singapore) and probe (Cole Parmer # V2-GG6-031, Singapore). The solution was left quiescent during both the initial salt saturation and back-extraction because the lenses tended to tear upon stirring. After the conductivity measurement, the wet lenses were removed from the vial, transferred to an oven at 50°C, and allowed to dry to a constant weight. The dry lenses were then placed in a vacuum desiccator to cool prior to weight measurement. The partition coefficients followed from eqs. (2) and (3). The results in Table II correspond to averages of at least five lenses in at least three separate experiments by two different

**TABLE II**
**Aqueous NaCl $k$ Values in the SCLs at 35°C**

| Trade name (FDA category)[a] | $w$ (wt %) | $k$ |
|---|---|---|
| Focus Night & Day™ (I/SiHy) | 24 | 0.15 |
| O2 Optix™ (I/SiHy) | 33 | 0.24 |
| PureVision™ (III/SiHy) | 36 | 0.26 |
| Acuvue Oasys™ (I/SiHy) | 38 | 0.31 |
| Biomedics™ 38 (I/H) | 38 | 0.38 |
| SofLens™ 38 (I/H) | 38 | 0.26 |
| Acuvue™ Advance (I/SiHy) | 47 | 0.37 |
| Biofinity™ (I/SiHy) | 48 | 0.33 |
| Clarity $H_2O$™ (II/H) | 54 | 0.32 |
| Biomedics™ 55 (IV/H) | 55 | 0.17 |
| Focus Monthly Visitint™ (IV/H) | 55 | 0.27 |
| Acuvue 2® (IV/H) | 58 | 0.32 |
| SofLens Daily Disposable™ (II/H) | 59 | 0.32 |
| Proclear™ One Day (II/H) | 60 | 0.55 |
| Proclear™ Sphere (II/H) | 62 | 0.44 |
| Focus™ Dailies (II/PVA) | 69 | 0.71 |
| SofLens One Day™ (II/H) | 70 | 0.70 |

[a] I (group I: nonionic, low $w$), II (group II: nonionic, high $w$), III (group III: ionic, low $w$), and IV (group IV: ionic, high $w$) give the FDA categories. H = HEMA; SiHy = siloxane; PVA = polyvinyl alcohol.

operators. The repeatability for a given operator is within 1%. Because of the blotting step, however, the percentage uncertainty between various operators can be up to 10%. Additional measurements were taken at several NaCl initial concentrations between 0.1 and 1*M*. Within the precision of the measurement, no difference in partition coefficient values was found.

### Permeation-cell design

We used the classic diaphragm-cell method, originally devised to measure solute diffusion coefficients in liquid solutions.[17–19] As illustrated in Figure 1, the permeation cell consists of two stirred compartments containing aqueous solutions of different salt concentration, separated by a single SCL. The lower compartment has the higher salt concentration; diffusion takes place through the lens because of the salt-concentration difference between the two chambers.

Aqueous NaCl transport in the permeation cell is due not only to diffusion across the lens but also to convective diffusion across the boundary layers adjacent to the lens in each compartment. Accordingly, a salt mass balance on each chamber, along with Fick's law for diffusion in the lens, gives[18,19]

$$\ln\frac{c_D(0)-c_R(0)}{c_D(t)-c_R(t)}=\ln\frac{\Delta c(0)}{\Delta c(t)}=\frac{\beta t}{R} \tag{4}$$

where $t$ is time, $c_D$ and $c_R$ denote the transient salt concentrations in the high-concentration donor (bottom) and the low-concentration receiver (top) reservoirs, respectively; β is the cell constant for a lens of exposed surface area $A$ inserted between the chambers of liquid volumes $V_D$ and $V_R$:

$$\beta=A\left(\frac{1}{V_D}+\frac{1}{V_R}\right) \tag{5}$$

and $R$ is the overall cell mass-transfer resistance:

$$R=\frac{1}{k_D}+\frac{L}{P}+\frac{1}{k_R} \tag{6}$$

where $k_D$ and $k_R$ are the mass-transfer coefficients in the stirred boundary layers of the donor (bottom) and receiver (top) reservoirs, respectively, and $P$ is the salt permeability of a lens of thickness $L$. Implicit in eq. (4) is the restriction that the aqueous salt solution is sufficiently dilute so that $P$ is constant and independent of NaCl concentration and that sodium and chloride ions diffuse together as a neutral species (i.e., $2D^{-1}=D_+^{-1}+D_-^{-1}$, where $D$ is the binary salt diffusivity, $D_+$ is the aqueous sodium-ion diffusivity and $D_-$ is the aqueous chloride-ion diffusivity[24]).

Equation (4) provides the means to ascertain the lens salt permeability: $P$ follows from the slope of a semilogarithmic graph of $\Delta c(0)/\Delta c(t)$ versus time provided that the cell constant, lens thickness, and mass-transfer coefficients are known. To account for the liquid-phase boundary-layer resistances, the overall mass-transfer resistance ($R$) in eqs. (4) and (6) is measured as a function of the stirring rate in the donor and receiver chambers. Over a wide range of impeller and agitator designs in the stirred tanks, Fletcher[25] reported that the mass-transfer coefficient scales as the impeller speed to the ⅔ power. Boher[26] confirmed this exponent for track-etched membranes of small pore sizes inserted between two stirred chambers. Thus, a plot of $R$ versus the inverse impeller speed to the ⅔ power is linear with intercept $L/P$.[27]

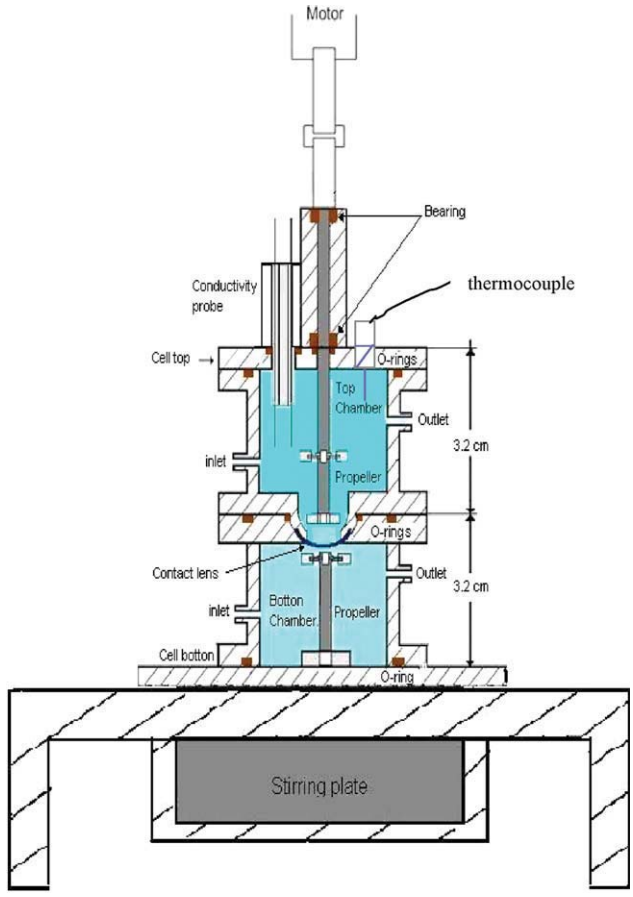


**Figure 1** Schematic of the aqueous NaCl permeability cell. [Color figure can be viewed in the online issue, which is available at wileyonlinelibrary.com.]

Strictly, eq. (4) holds in the pseudo-steady state[18,19] where linear NaCl concentration profiles through the lens adjust quickly to the changing salt concentrations in the donor and receiver chambers. Accordingly, the concentration data in eq. (4) must be measured at times larger than $L^2/D$ when pseudo-steady conditions apply. In addition, the permeation cell must be operated for a sufficient time to permit a precise determination of $\Delta c(t)$. For

example, for a 1% change in the concentration of the receiver cell, the experiment must last longer than $L(\ln 1.01)/\beta P$. Therefore, to permit a convenient experiment timescale, small cell volumes of near 20 mL were chosen in our permeation cell.

Figure 1 shows a detailed schematic of the salt permeation cell. The bottom donor and top receiving chambers are 3.2 cm long Plexiglas cylinders with an inside diameter of 3.2 cm and a wall thickness of 0.3 cm. Two Plexiglas flanges with inside diameters of 3.2 cm, outside diameters of 5.1 cm, and thicknesses of 0.6 cm are solvent-welded to the top of the upper chamber and to the bottom of the lower chamber. The other end of each chamber is constructed to house the contact lens. A 14-mm-diameter hollow spheroidal male embossment with an 8-mm base curve is machined above the thick Plexiglas base plate (5.1 cm in diameter and 0.6 cm thick) of the top receiving chamber. A mating female recession is machined into the corresponding top plate of the bottom donor chamber. Six symmetrically located threaded holes permit the joining of the top and bottom chambers.

The SCL is sandwiched between the male embossment and the female recession and tightly sealed by two Buna O-rings, one with an inside diameter of 1.6 cm and a thickness of 0.16 cm and the other with an inside diameter of 3.5 cm and a thickness of 0.16 cm. The diffusion area is established by a centrally located hole with a diameter of 8 mm drilled through the male and female lens holder. The permeation cell top is a thick circular Plexiglas plate 5.1 cm in diameter and 1.3 cm thick that supports the conductivity probe, the thermocouple, and the upper stirrer rod.

To stir the top receiver chamber, two homebuilt stainless-steel, four-bladed propellers 8 and 12 mm in diameter were mounted on the same stainless-steel shaft, which was 9.5 cm long and 0.3 cm in diameter. The small-diameter propeller was placed at the very bottom end of the shaft to improve mixing in the liquid-filled recess adjacent to the concave side of the SCL (Fig. 1). The large-diameter propeller was located 12 mm above the small one and provided mixing in the top chamber. Two 0.6-cm o.d. double-shielded precision bearings (#57155K365, McMaster-Carr, Los Angeles, CA) were mounted on a 1.5-cm-diameter, 3.8-cm-long Delrin stirrer-shaft support and placed over the permeation cell top. A Buna O-ring (i.d. = 0.3 cm, thickness = 0.16 cm) prevented contact between the top-chamber solution and the stirrer-shaft support. The stirrer shaft was joined to the drive shaft (o.d. = 1.3 cm, i.d. = 0.3 cm) of a 1/6-hp model 1Z851B Dayton permanent magnet direct-current motor through two coupling hubs and a Buna spider shaft coupling junction (#L-050, Lovejoy, Inc., Downers Grove, IL). A direct-current MM23101 Minarik controller (South Beloit, IL) allowed variation of the shaft speed, as measured by a type 1531 General Radio stroboscope (Concord, MA).

To stir the bottom donor chamber, we affixed a 1.9-cm-long by 0.5-cm-diameter Teflon-coated magnetic bar to a 0.9-cm-long, 0.3-cm-diameter shaft and capped it with a stainless-steel, four-bladed propeller 12 mm in diameter. A submersible stirrer unit (Cole Parmer #C-04636-50) connected to a multistirrer MC 301 Scinic controller (Tokyo, Japan) was used to alter the stirrer speed in the bottom donor chamber. The permeation-cell bottom is an 8.9-cm-diameter, 0.6-cm-thick Plexiglas disk.

Two 0.6-cm-long Plexiglas stubs with an inside diameter of 0.2 cm served as inlet and outlet ports for both the top and bottom chambers. A QG 20 FMI pump is used to fill the bottom chamber with salt solution and the top chamber with salt-free water through 0.16-cm-i.d. silicone-rubber tubing. The volumes of the filled chambers were determined by weighing with DDI water. Accordingly, the cell constant for the permeation cell, ($\beta$) is 0.052 $cm^{-1}$. The entire permeation cell was immersed in a constant-temperature bath controlled at 35 $\pm$ 0.1°C by a Cole Parmer Polystat temperature controller. To validate the temperature of the cell, an OMEGA HH509R thermocouple (Stamford, CT) was inserted in the aqueous solution close to the top of the receiver cell; this allowed continuous temperature monitoring on a personal computer. Stirring had no effect on the cell temperature.

A homebuilt microconductivity probe was designed to measure the salt concentration in the top receiving chamber. It consisted of two 0.5-mm-thick, 4.5-cm-long platinum wires, each inserted into a 3.8-cm-long glass capillary with an inside diameter of 1.1 mm and an outside diameter of 2 mm. After wire insertion, the glass capillaries were carefully melted onto the platinum wire. Two opposing platinum sheets, 6 $\times$ 5 mm, were joined to the ends of platinum wires and separated by a 5-mm gap. The electrodes were mounted in a Plexiglas support and attached to the permeation-cell top. Solution resistance was measured with a Gen Rad 1689 RLC Digibridge (Westbury, NJ). To minimize the sensitivity of the microconductivity probe to bridge frequency, the platinum electrodes were liberally platinized using a YSI 3139 kit. The conductivity probe was calibrated at 1 KHz and 1 V with 35°C aqueous sodium-chloride solutions of differing concentrations from 0.0005 to 0.2*M*. The RLC Digibridge was interfaced to a personal computer through a dedicated LabView program for automatic data collection. Care was taken to shield the connecting cable between the bridge and the conductance probe, a necessity when one measures low solution conductivities.

### Permeation-cell operation

To eliminate preservatives and disinfectants in the original lens-packaging solution, the contact lens was soaked in DDI water for at least 48 h with the

water renewed at least twice a day. Next, the 0.9 wt % aqueous NaCl donor solution was vacuum degassed twice at 35°C for 30 min to minimize subsequent bubble formation in the permeation bottom cell and possible obstruction of the SCL. The bottom donor cell was affixed to the support, and the Teflon-bar stirrer was inserted. Filling and emptying silicone flow lines were connected, and the degassed donor salt solution was pumped into the bottom donor cell. The contact lens was then draped over the convex surface of the top receiving chamber, and the top and bottom chambers carefully sealed. Any air bubbles that inadvertently remained in the filled bottom chamber were eliminated by additional flow of donor salt solution.

Once the bubbles were carefully expunged, the inlet and outlet silicone flow tubes of the top receiver chamber were connected to the fill the chamber with DDI water. The receiving cell top was affixed to the top chamber, and the stirring rod, conductivity probe, and thermocouple were attached. Additional DDI water was pumped to remove any air bubbles. The entire cell was then immersed in the constant-temperature bath, which was controlled at 35 ± 0.1°C (Cole Parmer Polystat). The stirrer motor was connected to the stirrer rod through the coupling hubs, and the conductivity probe was connected to the Digibridge by the shielded cable. The speeds of the motor and the Teflon stirring bar were each adjusted to 400 rpm, as gauged by the stroboscope. The cell was left to equilibrate thermally for 1 h, as confirmed by the monitoring thermocouple.

The salt permeability of Polymacon lenses increased by about 10% between 25 and 35°C. Thus, it was important to achieve thermal equilibrium. Because the characteristic time for a lens to reach the diffusion steady state was $L^2/D = 2$ min (with $L =$ 100 μm and $D = 10^{-6}$ cm$^2$/s), the initial 1-h equilibration period also permitted the contact lens to reach pseudo-steady-state salt permeation. Thereafter, the solution electrical resistance in the top chamber was recorded every minute for 2 h. Overall mass balance permitted calculation of the bottom-chamber transient salt concentration needed in eq. (4). Figure 2 presents typical data for an Acuvue-Oasys lens, plotted according to eq. (4). Here, the time zero corresponded to that following the initial equilibration period. The slope of the straight line gives $\beta/R$. Our data obey the predicted linear trend with a correlation coefficient of 0.99; this indicates a precision of better than 1%.

Once $R$ was determined at fixed bottom and top stirrer speeds, the bottom stirrer speed was increased to 600 rpm, and the system was allowed to equilibrate for 10 min. Again, electrical resistance measurements were taken in the top chamber every minute for 2 h. This process was repeated for a

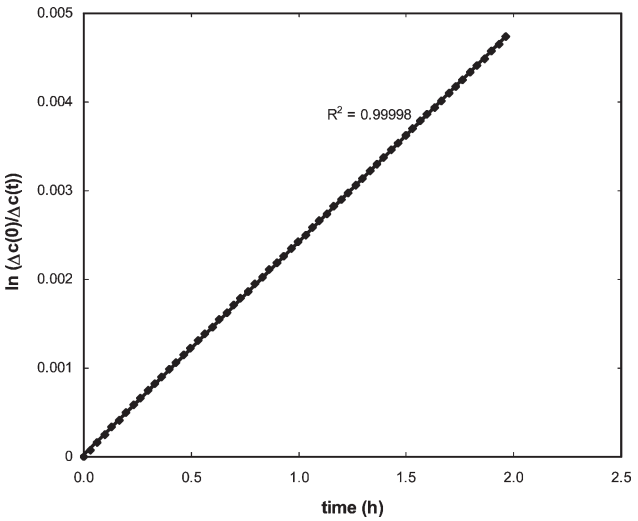


**Figure 2** Logarithm of the concentration change ratio in the NaCl permeability cell as a function of time for an Acuvue Oasys lens at 35°C and 400 rpm. The slope gives $\beta/R$ from eq. (4).

bottom stirring speed of 800 rpm. Next, the top-chamber motor speed was increased through 600, 800, and 1000 rpm at a constant bottom stirrer speed of 600 rpm. The electrical resistance as a function of time was similarly measured in the top chamber for each stirrer speed. The overall mass balance provided the bottom-chamber transient salt concentrations. To ensure reproducibility, each experiment was repeated twice with differing speed sequences and a fresh contact lens.

No variation of the overall cell mass-transfer resistance ($R$) with stirring speed was found in the bottom donor chamber for any of the SCLs studied. Therefore, the mass-transfer coefficient in the donor chamber ($k_D$) in eq. (6) was taken as infinitely large. Conversely, the effect of stirring speed in the receiving chamber was measurable, especially for lenses with aqueous NaCl permeabilities, which exceeded about $10^{-7}$ cm$^2$/s. To account for the mass-transfer resistance in the receiver chamber, we plotted the measured overall cell resistance as a function of the top stirrer speed to the $-2/3$ power, as explained previously. Figures 3 and 4 show examples for two of the lower and higher permeability lenses, respectively, and confirm the predicted straight-line behavior. The error bars on these figures correspond to the maximum difference between two repeat runs. The intercept of each line provides $L/P$ for that lens and, hence, yields $P$. Not only must the trend of $R$ with $\omega^{-2/3}$ be linear, but the slope must be identical for all lenses and lens types.[27] Our data confirm this assertion. Thus, the lines are best fit with the restriction that the slope for all lenses studied is identical. The reproducibility

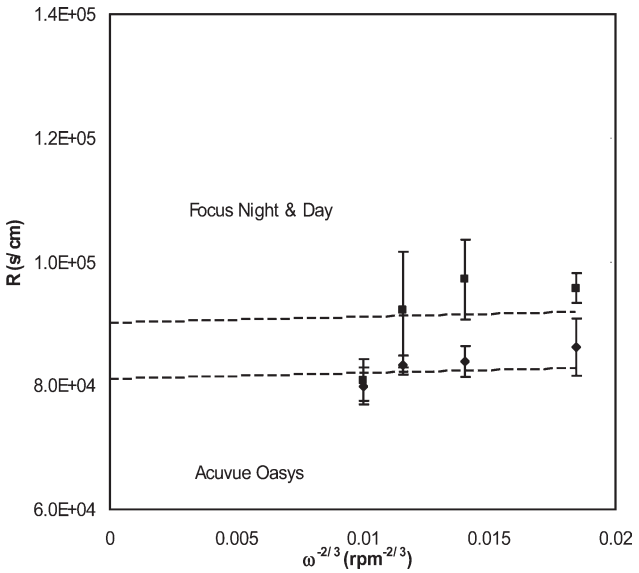


**Figure 3** Effect of the stirring speed in the top chamber on the overall cell resistance for two lower permeability SCLs. The intercept of the straight line gives *L/P*.

of the permeability values, including those from different operators, was less than ±7%.

In two sets of experiments, we utilized $10^{-3}$ and $10^{-2}M$ aqueous NaCl in the receiving chamber for PureVision lenses in addition to DDI water. The permeability obtained from all three measurements was $10^{-6}$ $cm^2/s$. This result supports the assumption implicit in eq. (4) that the dependence of permeability on salt concentration is not strong over the range studied.

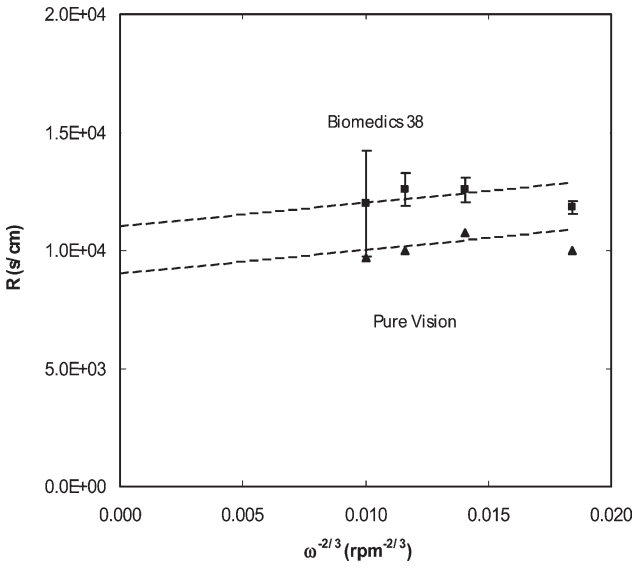


**Figure 4** Effect of the stirring speed in the top chamber on the overall cell resistance for two higher permeability SCLs. The intercept of the straight line gives *L/P*.

## RESULTS AND DISCUSSION

### Partition coefficients

Table II reports the newly measured aqueous NaCl partition coefficients (*k*) for 17 commercial lenses at 1*M* salt concentration (between 0.1 and 1*M*) and at 35°C. The results are the averages over at least three repeat experiments with at least two different operators. Figure 5 graphs the measured partition coefficients as a function of lens water content along with those available in the literature for SCL materials.[8,9,11,16] Squares indicate the commercial lens data measured here. Open symbols correspond to silicone-based materials (SiHy); filled symbols correspond to HEMA-based materials (H). Literature sources are given in the legend of Figure 5.

If neither salt ions nor water interact with the polymer matrix, the partition coefficient equals the saturated-water volume fraction in the lens.[9,10,21,22] When neither water nor salt interacts with the crosslinked polymer, the polymer component of the lens is invisible to both. Thus, ions and water in the lens matrix behave identical as in a bulk aqueous solution. In this noninteracting picture, $k = \varphi_1$, where $\varphi_1$ is the saturated volume fraction of water in the hydrogel. Because the mass densities of water and

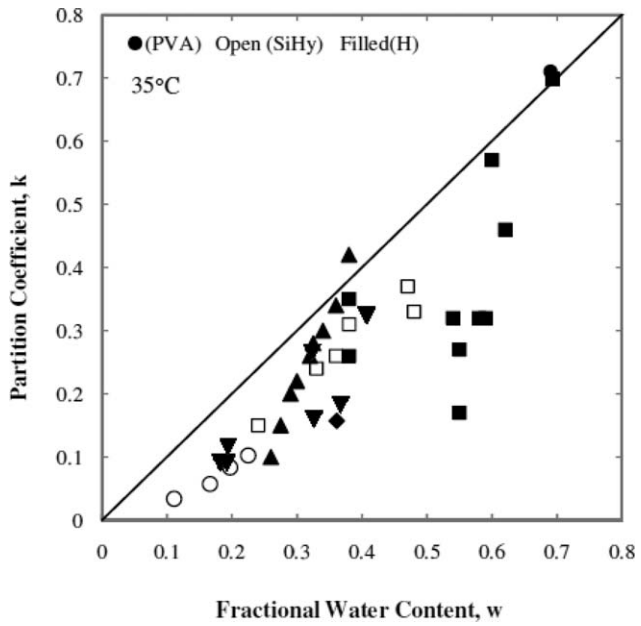


**Figure 5** Equilibrium partition coefficients (*k*) of 1*M* aqueous NaCl in SCL materials as a function of the equilibrium water content at 35°C: (●) PVA-based lens. The remaining filled symbols correspond to HEMA-based materials (H), whereas open symbols correspond to silicone-based materials (SiHy). (■ □) Commercial lenses from this study. All other symbols represent hydrogel membranes: (○) from Kim et al.,[16] (▼) from Yasuda et al.,[8] (▲) from Yoon and Jhon,[9] and (◆) from Hamilton et al.[11] The results of Yoon and Jhon[9] were measured at room temperature.

the polymer components are close, we replace the water volume fraction by $w$, the saturated mass fraction of water in the lens. Accordingly, a plot of $k$ versus $w$ should be linear with zero intercept and unity slope (i.e., $k = w$), as illustrated by the solid straight line in Figure 5.

The measured partition coefficients for essentially all of the commercial SCLs fall below the ideal partitioning line, in agreement with the findings of others for SCL materials.[8–12,16] Within experimental error, four commercial lenses obeyed the noninteracting linear relation with water content: Biomedics 38, Proclear One Day, Focus Dailies, and SofLens One Day. No distinctive behavior was seen for siloxane-based versus HEMA-based lenses. Four of the studied lenses (Acuvue 2, Biomedics 55, Soflens Daily Disposable, and Focus Monthly Visitint) exhibited exceptionally low salt partition coefficients, which are significantly below the solid line in Figure 5. Of these, three are classified as ionic lenses. This latter observation suggests that low partition coefficients might be attributed to charged groups decorating the polymer chains. To investigate this hypothesis quantitatively, we adopted Flory–Rehner–Donnan (FRD) theory,[28–32] as outlined in the first section of the Appendix.

FRD theory predicts salt partitioning in an aqueous polyelectrolyte due to nonspecific electrostatic repulsion between charged monomers in the polymer and the salt co-ion. Let $\kappa \equiv k/\varphi_1$ represent an enhancement factor for an aqueous solute in a hydrogel lens. A $\kappa$ less than unity corresponds to partial rejection of solute by the polymer matrix, whereas a $\kappa$ greater than unity indicates specific adsorption of solute to the polymer chains. Figure 6 shows $\kappa$ versus aqueous salt concentration on a log–log scale from FRD theory for a 1 : 1 strong electrolyte and for several molar charge fractions ($f_{[-]}$), in an anionic hydrogel. As outlined in the first section of the Appendix, the theory parameters are characteristic of a pHEMA/MAA copolymer. The calculated water content in Figure 6 is about 0.58, quite independent of salt concentration and the charged monomer molar fraction.

The enhancement factors in Figure 6 are always less than unity; this indicates partial salt rejection from the ionic hydrogel due to electrostatic repulsion. With only a few percentage of charged groups along the polymer backbone, $\kappa$ is orders of magnitude smaller than unity and dramatically so at low electrolyte concentrations. Thus, FRD theory predicts that ionic lenses exhibit concentration-dependent salt partition coefficients, depending on the magnitude of the matrix charge density. For salt concentrations of 0.1$M$ and lower, Donnan exclusion can explain the less-than-unity $\kappa$ values in Figure 5, even for relatively small charge densities. At $f_{[-]} = 1\%$, for

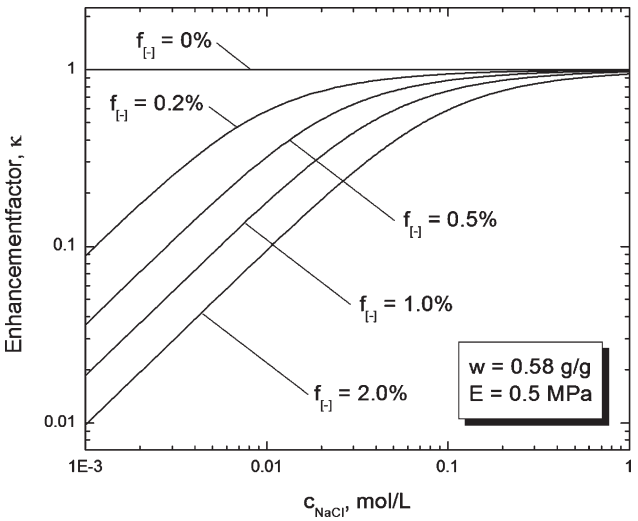


**Figure 6** FRD theory for the effect of the salt concentration on the aqueous NaCl enhancement factor ($\kappa$) for various polymer matrix charged monomer fractions $f_{[-]}$, expressed as a percentage. The parameters are those representative of the pHEMA/MAA copolymer, as described in the second part of the Appendix. The water content ($w$) varied minimally with added charge units and salt concentration. The nominal equilibrium water content is listed.

example, 25% of the salt is rejected from the hydrogel at 0.1$M$ salt concentration. At high salt concentrations near 1$M$, however, matrix charge is strongly screened, and the noninteracting model of $k = w$ emerges. Because the desorption experimental method adopted here to measure partition coefficients gauged $k$ corresponding only to the high-loading salt concentrations, Donnan electrostatic rejection does not explain partition coefficients lying below $k = w$ in Figure 5. More importantly, FRD theory cannot explain the low partition coefficients measured for the nonionic lenses.

Two further hypotheses may be offered to explain the partial rejection of salt from the lens materials shown in Figure 5. The melting of water frozen in hydrogels under differential scanning calorimetry (DSC) typically exhibits two broad endotherm peaks, one centered at 273 K and one extending down to about 240 K.[9,11,12,22,33–38] Although somewhat controversial,[35–37] the area under these two peaks, suitably scaled by the heat of fusion of pure water, gives the mass of free water in the hydrogel. The remaining water in the gel matrix is considered tightly bound to the polymer network and nonfreezable, presumably through hydrogen bonding with polar groups along the polymer chains.[33] DSC measurements of the mass of bound water vary depending on hydrogel composition, but typically range from 30 to 60%.[11,12,22,33–38] If one assumes there are between one and two water molecules tightly bound to a pHEMA repeat unit, a simple calculation, shown in

**TABLE III**
***P* and *D* Through SCLs at 35°C**

| Trade name (FDA category)[a] | *w* (wt %) | *P* ($10^8$ cm$^2$/s) | *D* ($10^6$ cm$^2$/s) | τ |
|---|---|---|---|---|
| Focus Night & Day (I/SiHy) | 24 | 12 | 0.80 | 5.11 |
| O2 Optix (I/SiHy) | 33 | 30 | 1.25 | 4.09 |
| PureVision (III/SiHy) | 36 | 100 | 3.85 | 2.33 |
| Acuvue Oasys (I/SiHy) | 38 | 7.8 | 0.25 | 9.11 |
| Biomedics 38 (I/H) | 38 | 25 | 0.71 | 5.41 |
| SofLens 38 (I/H) | 38 | 29 | 1.12 | 4.33 |
| Acuvue Advance (I/SiHy) | 47 | 76 | 2.05 | 3.19 |
| Biofinity (I/SiHy) | 48 | 130 | 3.94 | 2.30 |
| Clarity $H_2O$ (II/H) | 54 | 310 | 9.69 | 1.47 |
| Biomedics 55 (IV/H) | 55 | 120 | 7.06 | 1.72 |
| Focus Monthly Visitint (IV/H) | 55 | 240 | 8.89 | 1.53 |
| Acuvue 2 (IV/H) | 58 | 210 | 6.56 | 1.78 |
| SofLens Daily Disposable (II/H) | 59 | 251 | 7.84 | 1.63 |
| Proclear One Day (II/H) | 60 | 580 | 10.18 | 1.43 |
| Proclear Sphere (II/H) | 62 | 470 | 10.22 | 1.43 |
| Focus Dailies (II/PVA) | 69 | 600 | 8.45 | 1.57 |
| SofLens One Day (II/H) | 70 | 450 | 6.43 | 1.80 |

[a] I (group I: nonionic, low *w*), II (group II: nonionic, high *w*), III (group III: ionic, low *w*), and IV (group IV: ionic, high *w*) give the FDA categories. H = HEMA; SiHy = siloxane; PVA = polyvinyl alcohol.

the second section of the Appendix, gives the fraction of water in the hydrogel that is bound between 25 and 50%. If we posit that some[39] or all[11,12,22,33–38] of the bound water cannot hydrate salt ions, partition coefficients smaller than the equilibrium water content can be rationalized. Quantitative evaluation of the bound-water hypothesis, however, requires knowledge of the fraction of bound water ($f_{bw}$) available to solvate ions in addition to DSC melting endotherms; these are currently not available for the commercial lenses studied here.

The excluded volume ($V^{exc}$)[12] of salt ions in the hydrogel provides another hypothesis for enhancement factors less than unity. Solutes dissolved in the aqueous phase of the hydrogel can only approach the polymer chains to within their collision diameter. The region of closest approach to the polymer matrix not available to the solute molecules gives rise to an excluded volume. We do not include the additional excluded volume of the salt ions with each other in the aqueous volume fraction of the hydrogel because self-excluded volume is also present in the bulk aqueous phase and effectively cancels when the equilibrium partition coefficient is estimated. The third section of the Appendix provides a preliminary calculation of the effect of salt/polymer excluded volume on the partition coefficient for aqueous NaCl in pHEMA. We viewed the crosslinked polymer matrix as a cubic lattice laced by cylindrical strands. An excluded volume of about 20 % emerged. According to this simple estimate, the enhancement factor for NaCl in a HEMA hydrogel is 0.8. Except for high-water-content SCLs, most of the volume in the commercial lenses is occupied by polymer. Thus, salt/polymer excluded volume should not be neglected in models predicting equilibrium partitioning. A quantitative estimate of the salt/hydrogel excluded volume requires detailed knowledge of the polymer–matrix composition and architecture.

Bound water and excluded volume, especially when taken in concert, qualitatively explain the salt partition coefficients in nonionic SCL materials that are lower than the equilibrium water content. Without detailed information on the polymer composition and architecture, however, quantitative prediction is precluded. Although the matrix charge density may influence both bound water and excluded volume, the matrix charge is not required to understand less-than-unity enhancement factors. For ionic lenses, Donnan exclusion lowers *k* further. Thus, salt partition coefficients less than the water content of the gel are expected for both ionic and nonionic SCLs. Those lenses in Figure 5 whose salt partition coefficients are close to the solid line are apparent exceptions. For high-water-content lenses, the relative effects of bound water[33] and salt/polymer excluded volume diminish. For those lenses, enhancement factors should approach unity.

## Permeability

Table III reports the NaCl permeability (*P*) for the 17 commercial lenses investigated. Figure 7 shows on a semilogarithmic scale the aqueous salt permeabilities as a function of saturated water content for the commercial lenses shown in Table III and for lens materials from published results.[8,9,11–14,16] As shown in Figure 5, squares indicate the commercial-lens

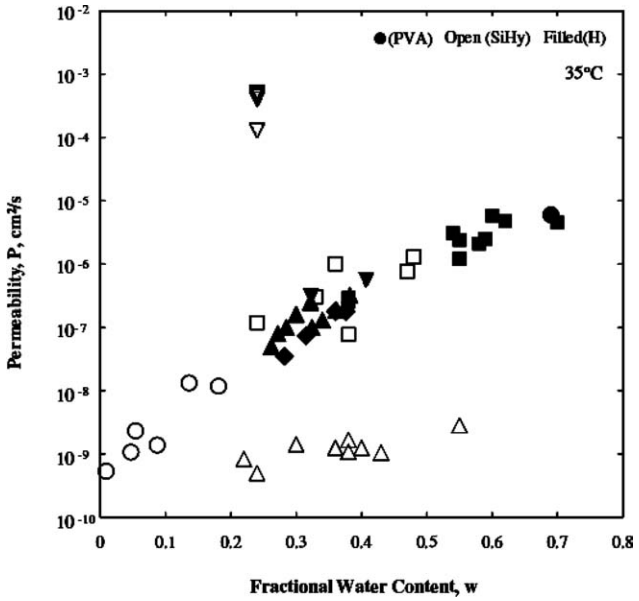


**Figure 7** Permeability ($P$) of aqueous NaCl in the SCL materials as a function of the equilibrium water content at 35°C: (●) PVA-based lens. The remaining filled symbols correspond to HEMA-based materials (H), whereas open symbols correspond to silicone-based materials (SiHy). (■ □) Commercial lenses from this study. All other symbols represent hydrogel membranes: (△) from Willis et al.,[13] (▽) from Weikart et al.,[14] (○) from Kim et al,[16] (▼) from Yasuda et al.,[8] (▲) from Yoon and Jhon,[9] and (◆) from Hamilton et al.[11] and Murphy et al.[12] The results of Yoon and Jhon,[9] Willis et al.,[13] and Weikart et al.[14] were measured at room temperature.

data measured here. Open symbols correspond to silicone-based materials (SiHy); filled symbols correspond to HEMA-based materials (H). Literature sources are given in the legend of Figure 7.

For the commercial lenses and most of the lens materials, there is a rough exponential increase of NaCl permeability with water content. This result confirms that NaCl transport occurs in the water phase of the gel. The exponential relation holds over a 4-order magnitude range of salt permeability, although some possible leveling is seen at the highest water contents. Whereas the salt partition coefficients vary by, at most, 1 order of magnitude, the salt permeabilities vary by many orders of magnitude over the same range of water contents. This observation highlights the importance of polymer architecture in salt diffusion through the hydrogels. Apparently, partition coefficients reflect primarily the gel composition, whereas the permeability strongly depends on gel structure in addition to composition. As with the salt partition coefficients reported in Figure 5, no distinct behavior is found for the siloxane-based versus the HEMA-based materials.

Two striking exceptions arise to the general exponential trend in Figure 7. Data from Willis et al.[13] fall 2 orders of magnitude below the general trend, whereas those from Weikart et al.[14] lie 3 orders of magnitude above it. For the same nominal materials and water contents, there is a 5- to 6-order magnitude difference in the salt-permeability measurements between Willis et al.[13] and Weikart et al.[14] Willis et al.[13] and, later, Kim et al.[16] indicate that their data were measured by the Ionoflux method[3] and, hence, correspond to the salt diffusivities. In the fourth section of the Appendix, however, we demonstrate that the Ionflux method gauges salt permeability and that the Stokes-cell method used here in eq. (4) and the Ionoflux method in eq. (A.11) must yield identical results. Therefore, the data from Weikart et al.[14] and Kim et al.[16] are plotted as salt permeability in Figure 7. Furthermore, the large discrepancies in Figure 7 cannot be explained by reporting the data as permeability rather than diffusivity because the aqueous NaCl partition coefficients are of order unity (see Fig. 5).

Salt-permeability measurements must be made with care. Our new data are in line with those of Yasuda et al.,[8] Yoon and Jhon,[9] Hamilton et al.,[11] Murphy et al.,[12] Kim et al.[16]

Nicolson and Vogt,[2] Hamilton et al.,[11] Willis et al.,[13] and Austin and Kumar[15] all indicated a percolation threshold for salt diffusion in crosslinked hydrogels. Below this threshold, the water phase no longer supports interconnected sample-spanning water paths that allow salt migration. In those studies, water contents below about 15 wt % did not permit salt diffusion. The concepts of bound water and salt/polymer excluded volume, discussed previously, are consistent with the hypothesis of a percolation threshold for salt migration. The data in Figure 7, however, report finite salt permeabilities for siloxane-based hydrogels with water contents as low as 2%, albeit very low permeabilities. It is conceptually possible for small amounts of water bound to the polymer matrix to transport salt ions along the polymer backbone. Only Kim et al.[16] examined the low-water-content regime shown in Figure 7. Further experiments are needed to address the issue of a salt percolation threshold for SCL hydrogels.

## Diffusivity

Table III also reports aqueous NaCl diffusivity ($D = P/k$) in the studied commercial lenses at 35°C. Partition coefficients are those from Table II. Also shown in Table III is the tortuosity ($\tau$) of each hydrogel established from the relation:[40]

$$D = D_0/\tau^2$$

where $D_0$ is the molecular self-diffusion coefficient of aqueous sodium chloride ($2.089 \times 10^{-5}$ at 35°C[41]).

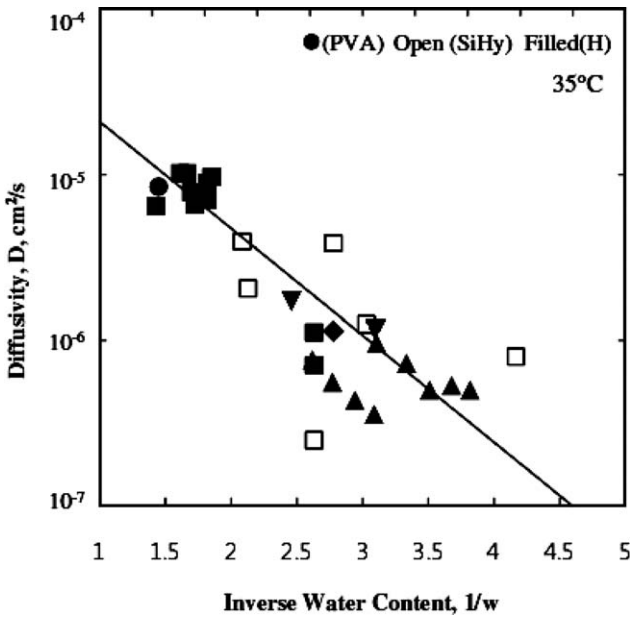


**Figure 8** Semilogarithmic graph of experimental aqueous NaCl diffusivity ($D$) versus inverse water content ($1/w$) from free-volume theory.[21] For $1/w = 1$, the diffusivity is that of aqueous NaCl at 35°C. The solid line guides the eye. (●) PVA-based lens. The remaining filled symbols correspond to HEMA-based materials (H), whereas open symbols correspond to silicone-based materials (SiHy). (■ □) Commercial lenses from this study. All other symbols represent hydrogel membranes: (▼) from Yasuda et al.,[8] (▲) from Yoon et al. (at room temperature),[9] and (◆) from Hamilton et al.[11]

The tortuosities decrease with increasing water content, as expected. For the lower water content lenses, $\tau^2$ is generally of order 10, although it can be as large as 100 indicating diffusion paths strewn with obstacles.

The simplest theory for $D$ in aqueous hydrogels is that of solute molecular jumps through accessible free volume in the water phase. The free-volume theory of Yasuda et al.[21] predicts a declining linear relationship between $\ln(D/D_0)$ and inverse water volume fraction. As discussed previously, we approximated the water volume fraction by water content (i.e., water weight fraction). Figure 8 displays the semilogarithmic plot of $D$ versus $1/w$ according to free-volume theory with the restriction that at unity water content, the diffusion coefficient is that of NaCl in water. The squares in Figure 8 correspond to the commercial lenses of this work. The remaining symbols represent available lens-material literature data. A solid trend line is shown. Although the data obey the general logarithmic decline of $D$ with increasing inverse water content, there are significant deviations from the theory of Yasuda et al.[21] Implicit in free-volume theory is that comparison is made to a homologous series of hydrogels differing only in water content. However, because Figure 8 compares widely different hydrogel materials, exact agreement with theory is not expected. An earlier study by Murphy et al.[12] for a homologous series of HEMA materials shows much better agreement with the theory of Yasuda et al.[21]

## CONCLUSIONS

Aqueous NaCl permeability, partition coefficient, and diffusion coefficient have been measured for a suite of commercial SCLs under physiological conditions. Permeability is measured by the Ionoton method in a miniature Stokes cell. We demonstrate that the so-called Ionoflux and Ionoton procedures for measuring permeability give identical results. Back-extraction of aqueous salt initially impregnated into lenses gives the equilibrium partition coefficient corresponding to the 1$M$ initial concentration. The permeabilities, partition coefficients, and diffusion coefficients of aqueous NaCl in commercial lenses all rise with increasing water content of the lenses. The permeabilities increase exponentially with water content, the partition coefficients increase approximately linearly, and the diffusivities decrease exponentially with inverse water content according to free-volume theory. The partition coefficients are smaller than the lens water content; they are rationalized for nonionic hydrogels by the presence of nonsolvating bound water near the polymer chains and by excluded volume between salt ions and polymer chains. For ionic lenses, there is also Donnan exclusion of salt ions from the lens matrix, especially at low salt concentrations. No distinctive behavior in $P$, $k$, or $D$ is found for aqueous NaCl diffusion through HEMA-based and siloxane-based SCLs or lens materials.

For help in the experiments, the authors thank B. P. Mahadik, G. Rosenthal, M. Joe, Y. Kim, A. Mekhdjian, C. Gollwitzer, T. Holland, and N. Myllenbeck.

## NOMENCLATURE

| | |
|---|---|
| $a$ | sum of the polymer chain radius and hydrated ion radius (Fig. 9; m) |
| $A$ | cross-sectional area for diffusion ($m^2$) |
| $c$ | molar concentration ($mol/m^3$) |
| $c_{[-]}$ | molar concentration of anionic monomers per unit volume of wet gel |
| $C_n$ | Flory rigidity factor |
| $d$ | hydrated-ion hard-sphere diameter (m) |
| $D$ | diffusion coefficient ($m^2/s$) |
| DDI | distilled/deionized water |
| DSC | differential scanning calorimetry |
| $E$ | Young's elongational elastic modulus (Pa s) |
| $f_{[-]}$ | mole fraction of charged repeat units in the polymer |

| | |
|---|---|
| $f_{bw}$ | fraction of bound water |
| FDA | U.S. Food and Drug Administration |
| FRD | Flory-Rehner-Donnan |
| H | hydroxyethyl methacrylate-based hydrogel material |
| HEMA | hydroxyethyl methacrylate |
| $J$ | molar diffusive flux (mol/m$^2$/s) |
| $k$ | partition coefficient of aqueous NaCl in the hydrogel |
| $L$ | harmonic mean thickness of the lens (m) |
| $l_{c-c}$ | carbon–carbon bond distance (m) |
| $M$ | molecular weight (g/mol) |
| $N_A$ | Avogadro's number |
| $N_{\text{mono}}$ | number of monomer repeat units per polymer chain |
| $P$ | permeability of aqueous NaCl in the hydrogel (m$^2$/s) |
| pHEMA | poly(hydroxyethyl methacrylate) |
| PVA | poly(vinyl alcohol)-based hydrogel |
| $r$ | cylindrical radius of a polymer chain (m) |
| $R$ | overall cell mass-transfer resistance (s/m) or the ideal gas constant (J mol$^{-1}$ K$^{-1}$) |
| SCL | soft contact lens |
| SiHy | siloxane-based hydrogel |
| $t$ | time (s) |
| $V$ | volume (m$^3$) |
| $V^{\text{exc}}$ | excluded volume |
| $\tilde{v}$ | molar volume (m$^3$/mol) |
| $w$ | saturated weight fraction of water in the hydrogel |

### Greek letters

| | |
|---|---|
| $\alpha$ | ratio of the NaCl partition coefficient at the final salt concentration to that at the initial concentration |
| $\beta$ | permeation cell constant (m$^{-1}$) |
| $\gamma$ | number of bound-water molecules per polymer repeat unit |
| $\kappa$ | enhancement factor |
| $\xi$ | mesh size (m) |
| $\rho$ | mass density (kg/m$^3$) |
| $\tau$ | tortuosity |
| $\varphi$ | volume fraction |
| $\chi$ | Flory chi parameter |
| $\omega$ | stirrer speed (s$^{-1}$) |

### Subscripts

| | |
|---|---|
| 0 | initial or bulk |
| 1 | water |
| 2 | polymer |
| $-$ | anion |
| $+$ | cation |
| $bw$ | bound water |
| $ch$ | chain |
| $D$ | donor chamber |
| $L$ | lens |
| $r$ | repeat |
| $R$ | receiver chamber |

## APPENDIX

### FRD theory

To investigate the role of lens charge density on salt partitioning into SCLs, we adopted FRD theory.[28–32] In this analysis, the SCL consists of crosslinked chains decorated with randomly dispersed and charged monomers, typical of a poly(HEMA-*co*-MAA) hydrogel. The hydrogel is equilibrated with an aqueous solution of known salt concentration. According to FRD theory, the phase equilibrium condition for the aqueous solvent in the presence of sodium chloride is

$$\ln \varphi_1 + \varphi_2 + \chi\varphi_2^2 + \tilde{v}_1 c_{\text{ch}}\left(\varphi_2^{1/3} - \varphi_2/2\right) + \tilde{v}_1\left[2c_{\text{NaCl}}(1-\kappa) - c_{[-]}/\varphi_1\right] = 0 \quad \text{(A.1)}$$

where $\varphi_1$ is the aqueous volume fraction in the gel and $\varphi_2$ ($= 1 - \varphi_1$) is the polymer volume fraction in the gel phase. We neglect the volume contribution of salt in the hydrogel. The symbol $\chi$ is the Flory parameter describing the interaction between water and the polymer, $\tilde{v}_1$ is the molar volume of water, $c_{ch}$ is the molar concentration of polymer chains in a dry network, $c_{\text{NaCl}}$ is the bulk molar aqueous salt concentration, and $\kappa$, the enhancement factor, is the ratio of the molar salt concentration in the gel divided by the bulk aqueous molar concentration of salt, each expressed per unit volume of water. Finally, $c_{[-]}$ is the molar concentration of anionic monomers per unit volume of wet gel. The first three terms in eq. (A.1) are those of Flory[28–30] and describe the behavior of the polymer and water. The fourth term reflects the elasticity of the crosslinked gel. Let $E$ denote the elongational Young's modulus of the water-saturated hydrogel. Because the gel crosslink density is directly proportional to the dry chain density ($c_{ch}$), Young's tensile modulus can be expressed as follows:[42–44]

$$E(\varphi_2) = 3RTc_{\text{ch}}\varphi_2^{1/3} \quad \text{(A.2)}$$

Equation (A.2) allows the calculation of the chain density in eq. (A.1) in terms of the measured Young's modulus of the hydrogel.[45] The factor of 3 on the right side arises because $E$ is a dilatational modulus rather than a shear modulus.[42,43] Dissolved salt is assumed to have no influence on the first four contributions in eq. (A.1).

The last term in eq. (A.1) corresponds to Donnan theory for salt partitioning in a polyelectrolyte.[31,32]

In the Donnan analysis, salt ions interact electrostatically with charged monomers in the polymer chains. To evaluate the charge density typical of ionic soft contact lenses, we express $c_{[-]}$ in terms of the mole fraction of charged monomer units in the network ($f_{[-]}$):[30]

$$c_{[-]} = f_{[-]}\varphi_2/\tilde{v}_r \tag{A.3}$$

where $\tilde{v}_r$ is the molar volume of the polymer repeat unit. In the case of a pHEMA/MAA hydrogel, the molar volumes of HEMA and MAA monomers are not substantially different; therefore, $f_{[-]}$ can be estimated by the weight fraction of MAA used in the gel synthesis.

Equations (A.1)–(A.3) contain two unknowns: water volume fraction ($\varphi_1$; approximately the water content) and enhancement factor ($\kappa$). Thus, we also must write the Donnan criterion for the equilibration of salt between a charged hydrogel and an aqueous phase:[31,32]

$$\kappa\left[\kappa + c_{[-]}/(c_{\mathrm{NaCl}}\varphi_1)\right] - 1 = 0 \tag{A.4}$$

Correction for electrostatic Debye–Hückel interactions[24] between salt ions in water is not taken into account in eq. (A.4), as these effectively cancel between the gel and aqueous phases. Equations (A.1)–(A.4) are solved using Newton iteration to obtain $\varphi_1$ and $\kappa$ as a function of salt concentration in the aqueous phase for various fractions of charged monomers in the hydrogel. The parameters adopted are those characteristic of pHEMA/MAA: $E = 0.5$ MPa,[45] $\chi = 0.66$, and $\tilde{v}_r = 0.102$ m$^3$/kmol.

As described in the text, Figure 6 gives the calculated enhancement factor as a function of salt concentration for percentages of charged MAA in pHEMA ranging from 0 to 2%. For Young's modulus values representative of SCLs[45] and with $\chi = 0.66$, the calculated nominal water content is 58%. We find little variation of lens water content with salt concentration, in agreement with the experimental values for pHEMA.[11] Also, the nominal water content is essentially independent of $f_{[-]}$ over the range considered in Figure 6.

### Estimate of bound water

A simple estimate of bound water is available as follows. Let $\gamma$ represent the number of bound-water molecules per repeat unit of the polymer. Then, the molar concentration of bound water per volume of wet lens ($c_{bw}$) is given by

$$c_{bw} = \gamma\rho_2\varphi_2/M_r \tag{A.5}$$

where $\rho_2$ is the mass density of dry polymer (1.274 g/cm$^3$ for pHEMA[20]) and $M_r$ is the molecular weight of a repeat unit (130 g/mol for pHEMA). The molar concentration of water in the gel is $\varphi_1/_1$, so the fraction of bound water relative to the total water in the hydrogel is the ratio of these two concentrations:

$$f_{bw} = \frac{\gamma\rho_2\varphi_2\tilde{v}_1}{\varphi_1 M_r} \tag{A.6}$$

From the molecular structure of HEMA, it is not unreasonable to assume between one and two water molecules are bound to each HEMA monomer. Thus, for a 40% water-content lens, we estimated $f_{bw}$ as about 25% for $\gamma = 1$ and 50% for $\gamma = 2$. Alternately, the fraction of bound water can be expressed per mass of dry polymer ($= \gamma\rho_1\tilde{v}_1/M_r$); this gave a value of about 28% for $\gamma = 2$, in excellent agreement with literature for pHEMA.[38] Our estimate is simplified as bound water may depend on the matrix charge density and on the water and salt contents, in addition to the salt type.[12]

### Estimate of excluded volume

Polymer physics provides an estimate of salt excluded volume in a hydrogel. The gel mesh size ($\xi$) is defined as the statistical length between two crosslinks.[46] Peppas et al.[47] quantify the mesh size as

$$\xi = l_{c-c}\sqrt{2C_n\frac{M_{\mathrm{ch}}}{M_r}}\varphi_2^{-1/3} \tag{A.7}$$

where $l_{c-c}$ is the length of a covalent carbon–carbon bond in the backbone (1.54), $C_n$ is the Flory characteristic ratio or rigidity factor (6.9 for HEMA[48]), $M_r$ is the molecular weight of a repeat unit, in our case HEMA (130 g/mol), and $M_{ch}$ is the average molecular weight of a polymer chain between two crosslinks. Because $M_{ch} = \rho_2/c_{ch}$, the gel mesh size is available from eq. (A.2) given the Young's modulus. For example, for HEMA with a Young's modulus of 0.5 MPa, the calculated mesh size is about 9 nm.

Picture a simple cubic network whose edge length is $\xi$. The volume of the unit cell is $V_{\mathrm{cell}} = \xi^3$. Each chain edge is approximated by a simple cylinder of radius $r$, as illustrated in the plan view of Figure 9. The volume of the cell not occupied by the polymer network is filled with water containing salt ions whose hydrated diameter we take as $d = 5$ Å. As indicated in Figure 9, the center of a hydrated ion cannot move in the entire water phase because of its self-volume. The excluded volume per edge of one unit cell is given by

$$V^{\mathrm{exc}} = \xi\pi\left(a^2 - r^2\right)/4 \tag{A.8}$$

where $a = r + d/2$ is the distance between an edge and the center of a hydrated ion. The factor of 4 in

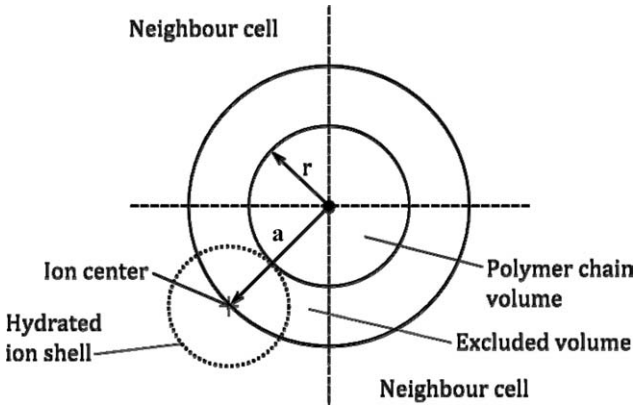


**Figure 9** End view of a single cylindrical polymer chain, illustrating the calculation of the ion/polymer excluded volume. The ion hydrated radius is $d/2$, and the polymer-strand radius is $r$. The excluded area is that of the annulus between radii: $a = r + d/2$ and $r$.

the denominator accounts for the sharing of the cylindrical volume among the neighboring cell, shown in Figure 9. To obtain the cylindrical radius of an edge polymer strand ($r$), we use the molar volume of a monomer in the polymer network ($\tilde{v}_r$). Thus, the cylindrical volume of a single chain is written as

$$\xi\pi r^2 = \tilde{v}_r N_{\text{mono}}/N_A \qquad \text{(A.9)}$$

where $N_A$ is Avogadro's constant and $N_{\text{mono}} = \rho_2/(c_{ch}M_r)$ is the number of monomer repeat units per polymer chain. $N_{\text{mono}}$ is calculated from Young's modulus of the gel through eq. (A.2). As there are 12 edges contributing to one cube, we obtain finally the ratio of excluded volume to water volume in the hydrogel:

$$\frac{\text{Excluded volume per elementary cell}}{\text{Total water volume per elementary cell}} = \frac{12V^{\text{exc}}}{\varphi_1\xi^3} \qquad \text{(A.10)}$$

According to this simple model, about 20% of the water phase is not accessible to the hydrated ions in a pHEMA lens. Other lens materials with higher moduli will have larger chain and crosslink densities. For higher chain densities, a larger fraction of salt in the hydrogel is excluded because the ratio of salt excluded volume to total water volume scales as chain density to the 3/4 power, per eqs. (A.7)–(A.10).

### Ionoton versus Ionoflux permeabilities

Nicolson et al.[3] present two methods to measure aqueous salt diffusion rates through SCLs. Their Ionoton technique is essentially that used in this work embodied in eq. (4) but without consideration of external mass-transfer resistance. In the Ionoflux method, early time concentrations in the donor chamber are measured as a function of time to establish the initial salt flux into that chamber. Nicolson et al.[3] claim that the Ionoflux method gauges the diffusion coefficient of salt in the hydrogel rather than the aqueous NaCl permeability. Accordingly, differing transport property values are obtained from the two techniques.[3] Because the Ionoflux method is said to require less time, it was adopted in several subsequent studies.[11–14,16]

To consolidate these two methods, we expand eq. (4) for a short time increment, $\Delta t < R/\beta$ and combine it with the overall salt balance:

$$V_D[c_D(\Delta t) - c_D(0)] + V_R[c_R(\Delta t) - c_R(0)] = 0$$

to give

$$V_R\frac{[c_R(\Delta t) - c_R(0)]}{\Delta t} = A[c_D(0) - c_R(0)]/R \qquad \text{(A.11)}$$

where $R$ is the overall mass-transfer resistance defined in eq. (6). The left side of eq. (A.11) is the rate accumulation of salt in the receiver chamber; the right side corresponds to the membrane area multiplied by the flux of salt through the membrane: $J = [c_D(0) - c_R(0)]/R$. Upon rearrangement, eq. (A.11) predicts a linear rise in the concentration of salt in the receiver chamber with time. The slope of that linear rise gives the aqueous salt permeability in the hydrogel,[11,12] provided that the mass-transfer resistances in the donor and receiver chambers are negligible or are accounted for. By assuming that $P = D$, Nicolson et al.,[3] Willis et al.,[13] and Kim et al.[16] utilized a rearranged form of eq. (A.11) to report aqueous salt diffusivities in SCLs. The analysis given here, however, indicates that because concentrations in the surrounding donor and receiver chambers appear in the analysis, salt permeability is measured. Hence, the values for $P$ obtained from the Ionoflux and Ionoton methods must be identical. For this reason, we plot diffusivity values reported by Willis et al.[13] and Kim et al.[16] as permeability values in Figure 7. We experimentally confirmed this conclusion by analyzing our data both by eqs. (4) and (A.11) to obtain identical values for $P$. However, the short-time analysis of eq. (A.11) can be subject to error when fewer data are collected. There is an additional restriction in eq. (A.11) that pseudo-steady-state salt diffusion applies in the lens or $\Delta t \leq L^2/D$, as for eq. (4).

### References

1. Silicone Hydrogels: The Rebirth of Continuous Wear Contact Lenses; Sweeney, D. F., Ed.; Butterworth-Heinemann: Oxford, 2000.
2. Nicolson, P. C.; Vogt, J. Biomaterials 2001, 22, 3273.
3. Nicolson, P. C.; Baron, P. C.; Charbrecek, P.; Court, J.; Domschke, A.; Griesser, H. J.; Ho, A.; Hopken, J.; Laycock, B.;

Liu, Q.; Lohmann, D.; Meijs, G. F.; Papaspiliotopoulos, E.; Riffle, J. S.; Schindhelm, K.; Sweeney, D. F.; Terry, W. L.; Vogt, J.; Winterton, L. C. U.S. Pat., 5,965,631 (1999).
4. Tighe, B. In Silicone Hydrogels: The Rebirth of Continuous Wear Contact Lenses; Sweeney, D. F., Ed.; Butterworth-Heinemann: Oxford, 2000; Chapter 1.
5. Tighe, B. In Silicone Hydrogels: Continuous Wear Contact Lenses; Sweeney, D. F., Ed.; Butterworth-Heinemann: Oxford, 2004; Chapter 1.
6. Sweeney, D. F.; Keay, L.; Jalbert, I.; Sankaridurg, P. R.; Holden, B. A.; Skotnitsky, C.; Stephensen, A.; Covey, M.; Rao, G. N. In Silicone Hydrogels: The Rebirth of Continuous Wear Contact Lenses; Sweeney, D. F., Ed.; Butterworth-Heinemann: Oxford, 2000; Chapter 5, p 90.
7. Domschke, A.; Lohmann, D.; Winterton, L. Presented at the ACS 213th National Meeting, San Francisco, 1997.
8. Yasuda, H.; Lamaze, C. E.; Ikenberry, L. D. Makromol Chem 1968, 118, 19.
9. Yoon, S. C.; Jhon, M. S. J Appl Pol Sci 1982, 27, 3133.
10. Yoon, S. C.; Jhon, M. S. J Appl Pol Sci 1982, 27, 4661.
11. Hamilton, C. J.; Murphy, S. M.; Atherton, N. D.; Tighe, B. J. Polym 1988, 29, 1879.
12. Murphy, S. M.; Hamilton, C. J.; Tighe, B. J. Polym 1988, 29, 1887.
13. Willis, S. L.; Court, J. L.; Redman, R. P.; Wang, J.; Leppard, S. W.; O'Byrne, V. J.; Small, S. A.; Lewis, A. L.; Jones, S. A.; Stratford, P. W. Biomaterials 2001, 22, 3261.
14. Weikart, C. M.; Matsuzawa, Y.; Winterton, L.; Yasuda, H. K. J Biomed Mater Res 2001, 54, 597.
15. Austin, D.; Kumar, R. V. Ionics 2005, 11, 262.
16. Kim, J.; Conway, A.; Chauhan, A. Biomaterials 2008, 29, 2259.
17. Northrop, J. H.; Anson, M. L. J Gen Physiol 1929, 12, 543.
18. Gordon, A. R. Ann N Y Acad Sci 1945, 46, 285.
19. Stokes, R. H. J Am Chem Soc 1950, 72, 763.
20. Polymers: A Properties Database; Ellis, B., Ed.; Chapman & Hall/CRC: Boca Raton, FL, 2000.
21. Yasuda, H.; Peterlin, A.; Colton, C. K.; Smith, K. A.; Merrill, E. W. Makromol Chem 1969, 126, 177.
22. Mirejovsky, D.; Patel, A. S.; Young, G. Biomaterials 1993, 14, 1080.
23. Peng, C. C. Private communication, 2009.
24. Newman, J.; Thomas-Alyea, K. E. Electrochemical Systems, 3rd ed.; Wiley-Interscience: Hoboken, NJ, 2004; Chapters 6 and 11.
25. Fletcher, P. Chemical Eng 1987, 435, 33.
26. Bohrer, M. P. Ind Eng Chem Fund 1983, 22, 72.
27. Chhabra, M.; Prausnitz, J. M.; Radke, C. J. Ind Eng Chem Res 2008, 47, 3540.
28. Flory, P. J.; Rehner, J. J Chem Phys 1943, 11, 512.
29. Flory, P. J.; Rehner, J. J Chem Phys 1943, 11, 521.
30. Flory, P. J. Principles of Polymer Chemistry; Cornell University Press: Ithaca, NY, 1953; Chapter XIII.
31. Donnan, F. G. Chem Rev 1924, 1, 73.
32. Overbeek, J. T. G. In Colloid Science I: Irreversible Systems; Kruyt, H. R. Ed.; Elsevier: Amsterdam, 1952; Chapter IV, p 188.
33. Tranoudis, I.; Efron, N. Contact Lens Anterior Eye 2004, 27, 193.
34. Pedley, D. G.; Tighe, B. J. Br Polym J 1979, 11, 130.
35. Mirejovsky, D.; Patel, A. S.; Rodriquez, D. D. Curr Eye Res 1991, 10, 187.
36. Peschier, L. J. C.; Bouwstra, J. A.; de Bleyser, J.; Junginger, H. E.; Leyte, J. C. Biomaterials 1993, 14, 945.
37. Phuong, Y. G.; Hill, D. J. T.; Whittaker, A. K. Biomacromolecules 2002, 3, 991.
38. Sung, Y. K.; Gregonis, D. E.; John, M. S.; Andrade, J. D. J Appl Polym Sci 1981, 26, 3719.
39. Higuchi, A.; Iijima, T. J Appl Polym Sci 1986, 32, 3229.
40. Chhabra, M.; Prausnitz, J. M.; Radke, C. J. Biomaterials 2007, 28, 4331.
41. Aseev, G. G. Electrolytes, Transport Phenomena: Methods for Calculation of Multicomponent Solutions and Experimental Data on Viscosities and Diffusion Coefficients; Begell House: Moscow, 1998; p 532.
42. Horkay, F.; Zrinyi, M. Macromolecules 1988, 21, 3260.
43. Stein, R. S.; Powers, J. Topics in Polymer Physics; Imperial College Press: London, 2006; Chapter 7.
44. Walowski, C. Private communication, 2010.
45. Tranoudis, I.; Efron, N. Contact Lens Anterior Eye 2004, 27, 177.
46. de Gennes, P. G. Scaling Concepts in Polymer Physics; Cornell University Press: Ithaca, NY, 1979; Chapter II.
47. Peppas, N. A.; Moynihan, H. J.; Lucht, L. M. J Biomed Mater Res 1985, 19, 397.
48. Peppas, N. A.; Moynihan, H. J.; Lucht, L. M. J Biomed Mater Res 1980, 19, 297.